Structure of inorganic nanocrystals confined within carbon nanotubes

Stefania Sandoval[*,†], *Gerard Tobias*[†], *Emmanuel Flahaut*[*,‡]

[†]Institut de Ciencia de Materials de Barcelona (ICMAB-CSIC), Campus de la UAB, 08193 Bellaterra, Barcelona, Spain

[‡]CIRIMAT, Université de Toulouse, CNRS, INPT, UPS, UMR CNRS-UPS-INP N°5085, Université Toulouse 3 Paul Sabatier, Bât. CIRIMAT, 118, route de Narbonne, 31062 Toulouse cedex 9, France

*Corresponding authors:

flahaut@chimie.ups-tlse.fr (E. Flahaut), ssandoval@icmab.es (S. Sandoval)

Abstract

There are many examples in which the cavities of carbon nanotubes have been filled with a variety of compounds. Unprecedented structures compared to those of the same material in the bulk are observed, such as low dimensional crystals. Such encapsulated materials can have unusual properties that differ from those of the bulk material. The scope of this review is to give a brief approach to the different nanostructures formed after encapsulation of inorganic compounds within the inner cavities of carbon nanotubes. The confined materials can take the form of one-dimensional nanowires, nanoclusters or even inorganic nanotubes. This review is part of the special issue of the journal dedicated to Prof. Malcolm L.H. Green, and special emphasis is thus given to the work performed by the group of Prof. Green.

Introduction

Carbon nanotubes are synthetic carbon allotropes composed by one (single walled-), two (double walled-) or more (multiwalled-) concentrically rolled-up layers of graphene. The morphological characteristics of the nanotubes can vary depending on the method of synthesis and growth conditions. Their width can range from 0.5 nm up to tens of nm (depending on the number of concentric layers) and they can reach centimeters in length. Their cylindrical shape and chemical structure (honeycomb carbon lattice) confer the material unique properties with potential applications in biomedicine,[1, 2] catalysis,[3] nanocomposites[4] or electronics.[5] Their range of application can be further expanded by the formation of hybrid materials via endohedral filling[6-9] or external decoration.[10, 11] The encapsulation at the nanoscale, which is the focus of the present review, allows tuning the properties of both the guest species that can undergo modifications of their space configuration, crystalline structure or the atomic ratio of their constituting elements[7] and the host, which electronic and optical properties can also be impacted due to the interaction between the new encapsulated material and the walls of the nanotubes.[8, 9] When discrete molecules of a material are confined inside the nanotubes their intermolecular interactions can be modified, compared to their bulk counterpart, leading to the formation of new nanostructures, resulting from rearrangements or chemical reactions between the confined species. CNTs can also play a protecting role, thus isolating the encapsulated material from the outer environment that can affect the final structure of the guest.[12, 13] Thus, different parameters might be taken into account for tuning the formation of specific nanostructures inside carbon nanotubes. The resulting structure depends on the chemical nature of the bulk material, steric factors or the presence of more than one species inside the nanotube (when chemical reactions occur within the host). The morphological

characteristics of the host also play an important role, since CNTs can have a wide range of diameters and lengths, affecting the space available for the formation of these new entities.[14, 15]

Different synthetic approaches have been proposed for encapsulating a wide number of species inside carbon nanotubes.[16] For both inorganic or organic species, the filling strategy depends on the properties of the guest, namely, crystal-nanotube interaction energy, melting point, viscosity, surface tension, vapor pressure, thermal stability or redox potential of the filler.[17] Filled carbon nanotubes can be prepared in one single step, *in situ* approach, when the inorganic catalyst used to promote the synthesis is simultaneously encapsulated inside the host. *In situ* approaches include arc-discharge, electrochemical and chemical vapor deposition methods and usually the processes lead to the encapsulation of metal or metal carbide nanoparticles and nanowires inside the carbon nanotubes.

Ex-situ approaches, namely, molten phase, gas phase and solution filling are more widely used since a larger variety of compounds can be confined inside the nanotubes, independently of their size or surface characteristics. This also allows to use specific nanotubes (number of walls, semiconducting or metallic, controlled chirality, purity, *etc.*) if this is relevant. However in the specific case of filling from solutions, low filling yields may be obtained and a preliminary treatment to open the ends of the carbon nanotubes is required to allow the diffusion of the species within their inner channels.[18]

The scope of this review is to give a brief approach to the different nanostructures formed after encapsulation of inorganic compounds within the inner channel of carbon nanotubes, with a special emphasis on the work performed by the group of Prof.

Malcolm L. H. Green. The effect of the morphology of the host and the filling method on the configuration of the new structure will be analyzed.

Selected examples of confined nanocrystals

The formation of nanocrystals resulting from the confinement of inorganic compounds inside carbon nanotubes have been widely documented. Unlike the *in-situ* approaches, with severe limitations in terms of controlling the resulting nanostructure, *ex-situ* techniques offer numerous alternatives for growing new crystalline entities with specific characteristics ruled by the chemical and physical properties of the inorganic precursor and the dimensions of the host nanotubes.[17] Confinement effects include a lowering of the coordination environment as well as distortions of the crystalline lattice or new rearrangements leading to the formation of low-dimensional materials inside the nanotubes that in some cases give rise to new crystalline structures. Depending on the filler / nanotube system and the experimental conditions, a wide range of morphologies from discrete nanoparticles / nanoclusters to 1D nanowires may be obtained.

Many efforts have been devoted to fill single-, double- and multi-walled carbon nanotubes with inorganic species. Usually, reports include the formation of crystalline nanoparticles and continuous nanowires, which structure is closely related to the method of synthesis. Using solvent-based techniques (solutions), nanotubes usually undergo partial filling of their cavities or the formation of discrete particles,[19, 20] probably due to the presence of solvation molecules that interfere in the growing of continuous structures within the nanotubes. Molten phase capillary wetting was proven as the most efficient technique for filling nanotubes with materials with surface tension below 200 mN/m.[21] First attempts to fill carbon nanotubes using this technique led to the formation of single crystals forming nanowires of metals,[22] metal oxides[23] and metal halides.[6]

In most cases, the encapsulation protocol involves using a large excess of filler (compared to the available space inside the nanotubes). During the filling procedure the

material not only crystallizes within the inner channels of the nanotubes, but also a significant amount of the inorganic precursor remains external to the carbon nanotubes.[24, 25] Since the presence of external material will generally interfere with the properties of the sample, further washing is required to clean the nanotubes. The washing conditions (solvent, temperature, time) depend on the nature of the filling material.[24] Having samples free of external material allows the quantitative determination of the encapsulated compounds.[26] It has been experimentally shown that the material encapsulated within narrow SWCNT and few-walled CNT by melt filling cannot be removed during the washing step, even when harsh conditions are involved.[25, 27] This is because the ends of the CNTs close upon cooling, thus inhibiting the dissolution of the crystals.[28] The temperature required to provoke the spontaneous closure of the CNT ends is diameter dependent, and high temperatures are needed to seal filled MWCNTs (ca. 1200 ºC).[29] In contrast, when low temperature routes are employed, such as solution filling, the ends of the nanotubes remain opened. Having opened ends allows to use filled nanotubes as carriers and to activate the discharge of their content in specific conditions, such as a pH variation.[30, 31] Failure of the guest to dissolve from open-ended CNTs may be indicative of a strong host-guest interaction or of the difficulty of forming an effective solvation sphere within the confines of narrow capillaries.[27] When containment of the guest is desired, fullerenes can also be used to cork the open-ends of CNTs.[32]

One important parameter to be considered for the template-assisted growth of nanomaterials is the inner diameter of the host. Meyer et al. carried out extensive studies of the influence of the inner dimensions of the carbon nanotubes on the crystalline structure of 1D materials obtained after molten phase filling of KI.[33, 34] Using high resolution transmission electron microscopy (HRTEM) and by means of through focal

series reconstruction, the authors determined the structure of the crystal encapsulated within SWCNTs of different diameters. The structure of the confined KI nanowires exhibit a preferred orientation with the <001> direction parallel to the tube axis, which is in agreement with the structure obtained when KCl was encapsulated within MWCNTs.[35] In all cases the thickness of the crystalline material was found to be ruled by the inner diameter of the tubes. Figure 1 shows the schematic representation (a)-1) and phase image (a)-2) of KI nanowires encapsulated within ca. 1.4 nm and 1.6 nm in diameter SWCNTs, respectively. While narrower SWCNTs (<1.4 nm) encapsulate two-layered KI crystals, 1.6 nm in diameter SWCNTs can encapsulate up to five layers containing one, two or three atomic columns (cross section) of I or K.

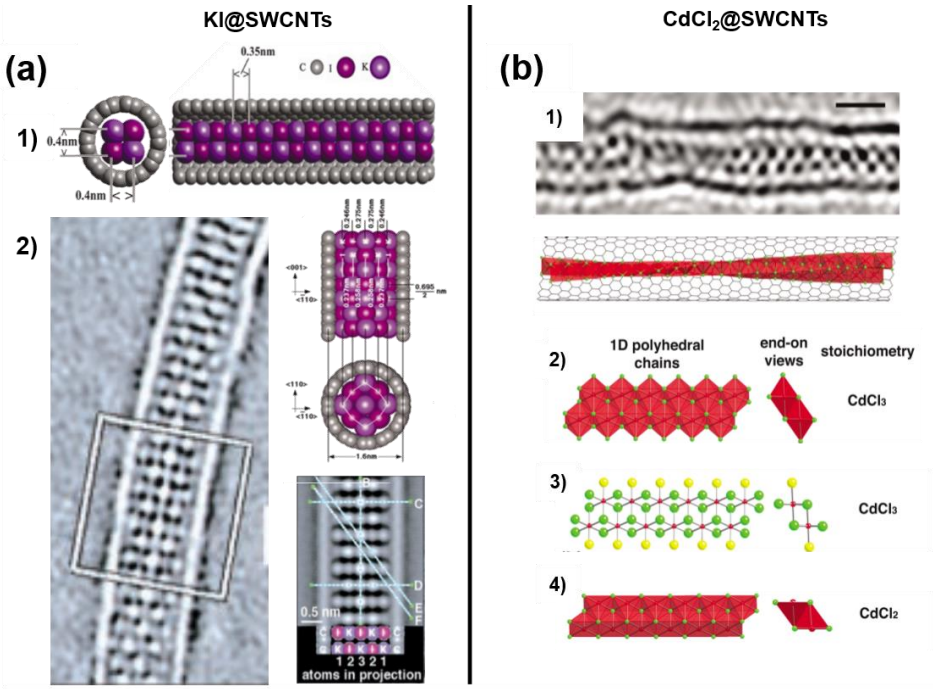

Figure 1. Structures of KI and $CdCl_2$ crystals encapsulated within SWCNTs*. (a) KI@SWCNTs: 1) Schematic representation of the 2x2 structure formed after encapsulation of KI within a 1.4 nm-width SWCNT. 2) HRTEM image of KI filled within a SWCNT (1.6 nm). The crystalline structure formed by five alternating layers (I-2K-3I-2K-1I or K-2I-3K-2I-K) undergoes lattice distortions that increase the interatomic distance in <110>. Adapted with permission from ref. [34], Copyright © 2000, The American Association for the Advancement of Science. (b) $CdCl_2$@SWCNTs: 1) Twisted 1D polyhedral chain formed after the preparation of $CdCl_2$@SWCNTs. The expected octahedral system 2), 3) was replaced by a square pyramidal structure 4) due to the removal of satellite Cl atoms. Adapted with permission from ref. [36], Copyright© 2002, The Royal Society of Chemistry.*

Although that the observed crystals have all been resolved as single KI unit cells viewed along different directions, lattice distortions were observed when compared to the parent rock salt structure. Since the electronic environment varies more drastically at the edges of the encapsulated structure, atoms located at the faces and corners undergo a reduction in their coordination degree from 6:6 (bulk crystal) to 5:5 or 4:4 according to the case. While the two layered structure confined within 1.4 nm SWCNTs can only present the 4:4 configuration, in case of the five layered structure all of them can be observed depending on the position of the atoms.

The variations of the crystalline structure accompanied by the interaction with the van der Waals surface of the host (CNT inner wall) are responsible of both the longitudinal contraction and the expansion in the cross section observed in the three layered structure. Similar structural variations are observed after filling other metal halides,[36] such as $TbCl_3$, which structure varied from a UCl_3-type to $CdCl_2$ –like system after encapsulation within SWCNTs (1.6 nm).[6] Other examples include changes of the orientation of the crystals due to the bending of the nanotubes, which might lead to the formation of new arrays of metal halides that cannot be associated to the bulk structure of the material[6] or the formation of new 1D polyhedral structures. Figure 1 (b) shows a nanocrystal of $CdCl_2$ inside a SWCNT prepared by the molten phase capillary wetting approach. A twisted 1D chain was obtained after growing the crystal inside the confined space (b)-1). Considering the 2D layered bulk structure of the salt, the formation of a 1D $CdCl_3$ polyhedral chain would have been expected (b)-2), -3). However, as in the case of KI the confinement induces a reduction of the coordination state, leading to the formation of a square pyramidal shape resulting from the elimination of Cl atoms from the edges (b)- 4).[37]

One interesting case is the encapsulation of BaI_2 within SWCNTs (Figure 2 (a)). In bulk, the structure of this alkaline earth metal halide is ruled by the pressure, adopting two different 9-coordinated and one 10-coordinated 3D forms. However, as in case of KI a reduction of the dimensionality is observed when confined within the nanotubes and the material adopts a configuration totally different to that of its bulk form. The resulting 1D polyhedral chain consists on a 1-2-3-2-1 system (a)-3) where Ba atoms (pink spheres, (a)-4) adopt both the octahedral (centre) or the pentagonal (edges) coordination, depending on the position of the atoms, similarly to the examples mentioned above. The formation of a novel structure of BaI_2, totally different from those previously reported, highlights the potentiality of CNTs for acting as directing templates for the formation of new crystalline entities at the nanoscale.

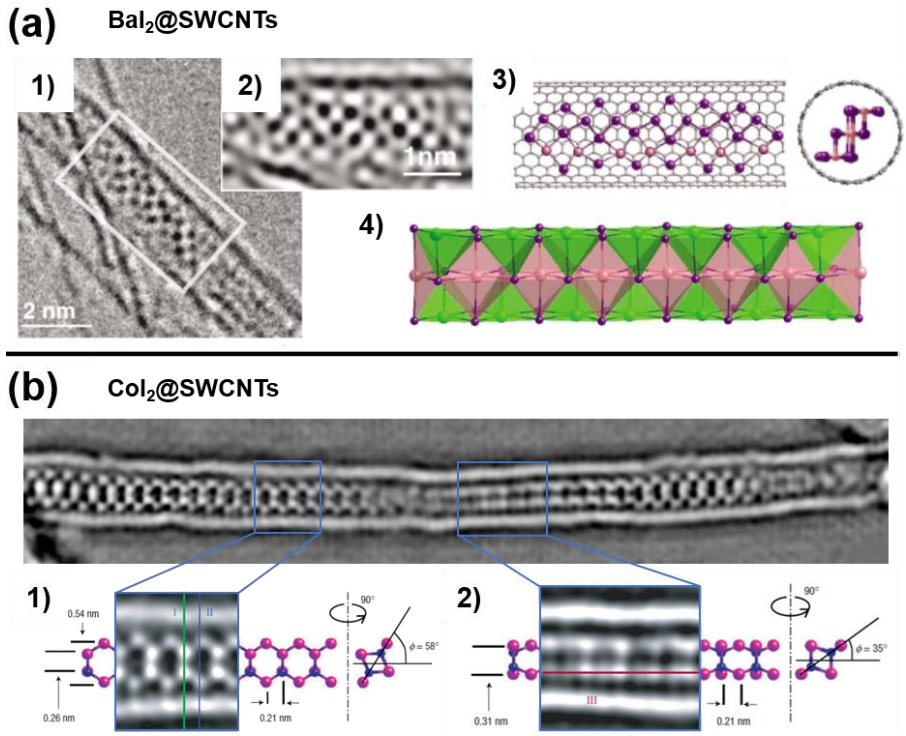

Figure 2. Structures of BaI_2 and CoI_2 crystals encapsulated within SWCNTs. *(a) BaI_2@SWCNTs: 1) 1D polyhedral chain of BaI_2 encapsulated within a 1.6 nm-diameter SWCNT. A magnification of the selected area (white square) is shown in 2). 3) side-on and end-on views of the one-dimensional nanostructure confined within the nanotube. 4) Ba atoms located at the edges adopt a pentagonal configuration while the atoms located at the centre are octahedrically coordinated to the I atoms. Adapted with permission from ref. [38], Copyright © 2002 John Wiley and Sons. (b) CoI_2@SWCNTs: Helical structure formed by 1) double chains of CoI_4 (tetrahedral structure) that rotates (23º) to adopt a rectangular arrangement in 2). Adapted with permission from ref. [39], Copyright © 2003, Springer Nature.*

The structure adopted by the guest can affect considerably the morphology and electronic properties of the nanotubes.[40] Philp *et al.* synthesized a helical nanostructure of CoI_2 that differed from the 2D organization of the bulk, after recrystallizing the molten salt within SWCNTs. Figure 2 (b) shows a continuous chain of CoI_2 encapsulated inside a SWCNT where two regions with different structures can be observed. The authors determined the structural model corresponding to the selected areas (b)-1) and (b)-2). In the first case, the higher intensity of the spots located at the column *I* suggests the superposition of cobalt and iodine atoms, in contrast to the lower intensity of the single atoms located along *II*. Thus, they proposed that each Co atom is tetrahedrally coordinated forming double chains of CoI_4. Unlike the first area, in (b)-2) the higher intensity signal is located along the tube axis and an apparent narrowing of the distance of the atoms located at the perpendicular direction to this axis was observed. The higher intensity spots alternate with weaker signals, again corresponding to single I atoms located between columns of superimposed Co-I atoms. This was explained by a 23º rotation or "twisting" of the initial structure, leading to a rectangular arrangement. Different degrees of rotation (helical rotation) are observed along the continuous chain encapsulated in the nanotube (Phase image, Figure 2 (b)) that can be closely related to the variations in the diameter along tube. The twisting effects of the new nanostructure might be able to distort the electron mobility along the surface of the nanotubes that contains it, since it was proven that both the host and the inorganic guest interact in a very close manner.

Not only metal halide nanocrystals have been reported inside the cavities of CNTs. Carter et al. studied the correlation between the novel 1D-structure of HgTe, formed after encapsulation in CNTs. The electronic modifications as well as the stability of the synthesized system were also investigated. Figure 3 (a)-1) shows an image of

HgTe@SWCNTs which corresponds to the presence of an orthogonal structure containing two layers of Hg_2Te_2 forming a Hg_4Te_4 motif. Additional constructions where the systems adopt different orientations regarding to the electron beam incident direction were observed. By varying both the local rotation angle regarding to the incident light and the internal Hg-Te-Hg angles (a)-2), the authors were able to determine the full three dimensional structure. Theoretical models were in agreement with the experimental data (a)-3), even in the case of tubes being tilted if compared to that initially observed (a)-4). The 1D HgTe nanostructure grown experimentally inside the tube shows significant modifications in its electronic properties, becoming semiconducting, compared to the bulk structural configurations (sphalerite and wurzite), which have semimetallic character.[41]

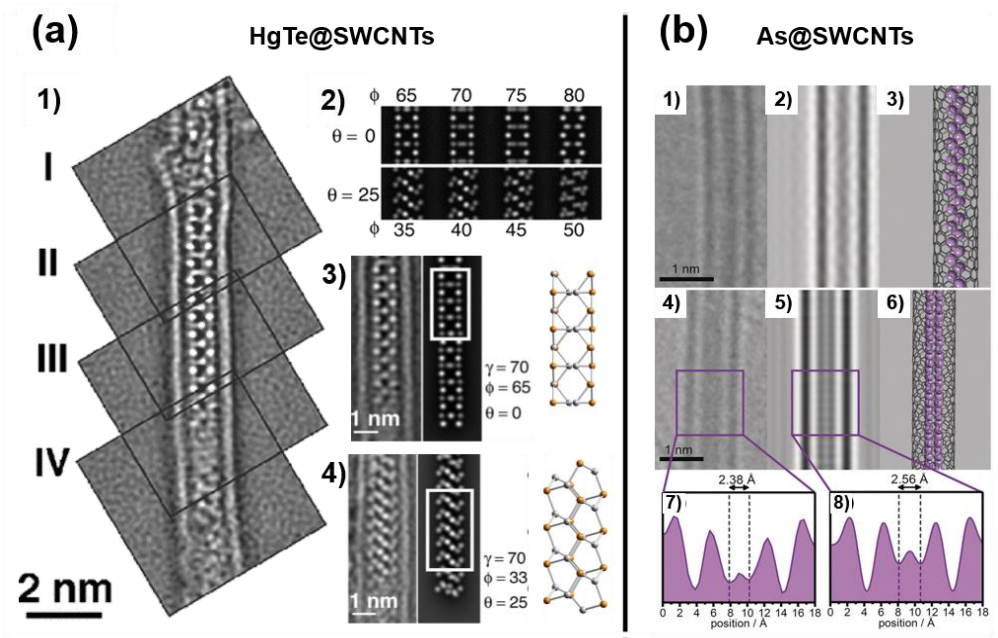

Figure 3. ***Structures of HgTe and As crystals encapsulated within SWCNTs****. (a) HgTe@SWCNTs: 1) Composite restoration of the phase of the exit plane wave function of one 1.36 nm- nanotube containing HgTe crystallite. 2) structures derived from simulations of motifs showing tilting angles of 0º and 25º and different local rotation angles. 3) A detail of the images in 1) showing that the structure corresponds to the simulated nanostructure with an interatomic angle (γ) Hg-Te-Hg of 70º. 4) The experimental image matches to the model theoretically proposed of a structure tilted with respect to 1). Adapted with permission from ref. [41], Copyright © 2006, The American Physical Society. (b)As@SWCNTs: HRTEM images, HRTEM simulations and proposed structures of 1-3) As zig-zag chain and 4-6) As zig- zag ladder confined within SWCNTs. The gap between the two ladders observed in the experimental line profile 7) match with theoretical predictions 8). Adapted with permission from ref. [7], Copyright © 2018, John Wiley and Sons.*

Monoelemental chains adopting a wide variety of structures have been also reported. Template-assisted synthesis of carbon allotropes,[42, 43] polymeric or ring shaped-phosphorus[44, 45] and iodine chains[46] are some examples of using CNTs to prepare new low-dimensional crystals. Using a vapour phase technique, Hart et al. were able to grow 1D arsenic nanostructures within SWCNTs. (Figure 3 (b)) The employed approach allowed the confinement of As_4 and two novel allotropic systems, namely, single stranded zig-zag chains (b)-1) and double stranded zig-zag ladders (b)-2). The final structure is closely related to the diameter of the host. The zig-zag ladders were found to prevail above the other structures. Thus CNTs were found to play a double role, acting not only as a template but also as a protecting agent to stabilize the new structures that might be highly reactive.[7]

Computational methods provide valuable information to predict the structure, filling behavior, template effects and interaction of the inorganic guests with the nanotubes.[47] In fact, most of the examples highlighted in this review were supported by theoretical investigations.[48] Novel structures have also been predicted using computational methods, as in the case of the encapsulation of CuI inside narrow CNTs. Here, two scenarios were considered: (i) taking into account that Cu^+ and Hg^{2+} have similar electronic configurations it seemed plausible the formation of a structure analogous to that formed by HgTe with a 3:3 coordination or (ii) since CuI adopts a rock salt structure under high pressure conditions (10 GPa), the formation of a 4:4 coordinated structure (derived from the NaCl rock structure) could take place. The resulting structures are presented in Figure 4 (a) which correspond to the geometry optimization from (i) and (ii). In both cases Cu atoms are located in the center, forming a chain where each Cu shares two I atoms located at the edges. However, the structure depicted in 1) showed the lower energy values and was selected for modelling the CuI

encapsulated within SWCNTs of different diameters, namely 10.85 Å, 12.36 Å and 13.56 Å. The spontaneity of the encapsulation process was directly proportional to the width of the tube, CuI undergoing a compression of its crystalline structure. [40]

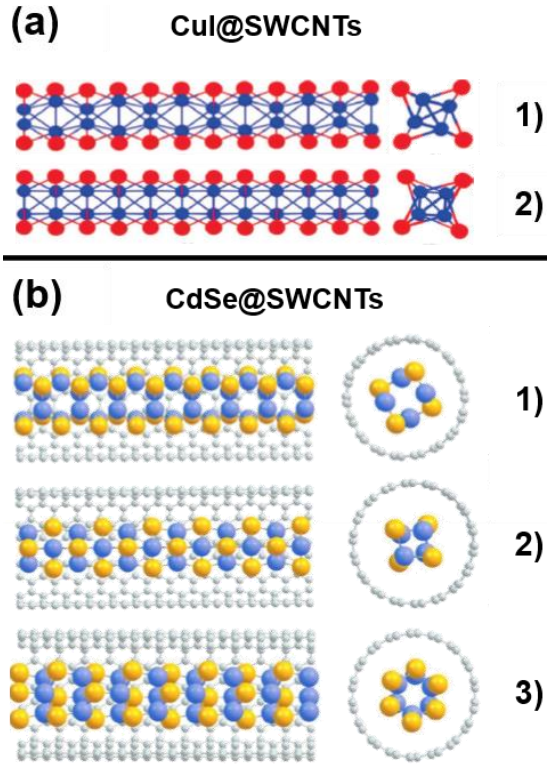

Figure 4. Predicted crystal structures of CuI@SWCNTs and CdSe@SWCNTs. (a) Optimized geometries of CuI encapsulated within small diameter carbon nanotubes. Adapted with permission from ref.[40], Copyright © 2008, The Royal Society of Chemistry. (b) Optimized 1) 3:3, 2) 4:4 and 4:2 coordinated CdSe structures resulting from encapsulation of CdSe inside SWCNTs. Adapted with permission from ref. [49], Copyright © 2018, John Wiley and Sons.

Kiselev et al. were able to encapsulate 1D crystals of CuI within SWCNTs[50] and subsequently determined experimentally the influence of the diameter of the host in the resulting structure of CuI encapsulates. Using 1.3-1.5 nm diameter arc-discharge SWCNTs and supported by theoretical calculations the authors identified the CuI hexagonal 3D bulk structure with a lowered dimensionality (by removal of peripheral atoms) and grown in the (001) and (1-10) directions parallel to the SWCNTs axis. The growth direction is closely related to spatial confinement effects. When a wider range of diameters was studied, microscopic observation led to consider that the CuI adopted two different types of crystalline structures: the 3D fcc crystal γ-CuI zinc blende (ZnS) and

the 3D crystal α-Cu rock salt (NaI) structural type. In order to encapsulate CuI crystals inside the SWCNTs (CCVD) with diameters ranged between 1.5 nm and 2 nm a half period translation of both types of structures was suggested. In case of the tetrahedral model (ZnS), which suffers a reduction of the number of the completely coordinated sites (from six to 1) after filling, a distribution of the atoms required for maintaining the stoichiometry was observed, accompanied by coordination of the peripheral copper atoms with the CNT host wall, which would stabilize their incomplete coordination. More drastic changes in the atomic distribution are required for encapsulation of the octahedral crystal (NaCl). In this case the fulfilling of the crystal stoichiometry can be obtaining either by filling outer cation positions or by removal of an iodine atom of the structure. However, the chosen option depends entirely of the diameter of the carbon nanotube. Finally, a 3D structure was observed after filling wider nanotubes (d >2 nm). Unlike the examples mentioned above, although the crystal maintains the (110) growth direction, the larger inner cavity of the nanotube allows the formation of more than one crystalline unit cell chain.[51]

Interatomic distances decrease with the diameter of the nanotube whereas the charge transfer between the hosting nanotube and CuI shows the opposite trend.[40] As mentioned above, both spatial confinement effects and stoichiometric deviations in the crystals encapsulated within narrow nanotubes may favor the chemical interaction between the inorganic guest and the CNT walls.[52] Electronic variations in the structure of the grown CuI nanostructure, reflecting interactions of its valence electron with the conjugated system of the CNT walls, as well as evidence of distortions of the tetrahedron environment of Cu ions by iodine atoms were detected by analyses of the X-ray absorption spectra of the samples.[53, 54] Otherwise, the encapsulation of CuBr within both metallic and semiconducting nanotubes provokes

downshifts in the C1s binding energies (as determined by X-ray photoelectron spectrospy) when compared to pristine nanotubes. The observed changes can be attributed to charge transfer from the nanotube to the 1D crystal due to the presence of Cu vacancies. Chemical and Fermi level shifts are significantly enhanced when studying nanotubes with narrower diameters (1.1-1.3 nm) due to the increased interaction of the crystal with the CNT host and evidence of the CuBr coupling with the nanotube was presented.[52] This behavior has been also observed when growing CuI and CuCl within SWCNTs, the interaction with the host been proportional to the electron affinity of the halogen atom, namely, CuI@SWCNT< CuBr@SWCNT < CuCl@SWCNT. Both the electron affinity and the anion size play important roles in the 1D crystal diameter, CuX-SWCNT interaction, stability and distortions in the crystalline structure of the guest.[55]

As a consequence of the crystal-CNT interaction, the electronic structure of carbon nanotubes suffers significant alterations. In order to determine filling induced changes in the electronic properties of the hosting SWCNT Kharlamova et al. evaluated both pristine (metallic) and AgCl@SWCNTs using Raman spectroscopy.[56] Variations in the RBM band of filled CNTs when compared to their empty counterparts suggest changes in the resonance excitation conditions due to deformations of the cross section of the host. Moreover, the upshifting and modification observed in the G-band confirm charge transfer between the nanotubes and the AgCl encapsulated crystals as well as doping and modification of the metallic to semiconducting character by gap opening in the band structure of filled nanotubes. In the same way, a transition in electrical transport features from hopping to weakly activated conduction by HgTe filling and also semi-metallic conduction in selenium-filled DWNT was also evidenced by

Chimowa et al, opening the way to a possible tuning of the transport properties of carbon nanotubes through filling.

Computational techniques are also useful to determine the crystal structure of materials experimentally filled, but this is often difficult due to the presence of light atoms that cannot be discerned by microscopic techniques. Figure 4 (b) shows the elucidated structures of CdSe@SWCNTs. In this case, X-ray diffraction and computational approaches were necessary to determine the morphology of the crystals. Using previous references, the authors proposed structures analogous to the 3:3 coordinated HgTe (b)-1), the NaCl rock salt (4:4, (b)-2) and a 4:2 CuI confined within CNTs.[50] After geometry optimization, the 3:3 coordinated model was established as the lower energy model, which also showed larger similarities when compared to the experimental results.[49]

As illustrated above, the interaction between the host and the guest usually leads to distortions of the guest in order to fit within the available space offered by the inner channel of the nanotubes. However, in the case of SWNTs, the nanotube itself may be distorted due to the crystallization of the host. This was evidenced in the case of CoI_2@SWNT [26] as discussed earlier. However, it is also possible, taking this the other way round, that the guest may not be allowed to crystallize if the inner space is too small and the distortion of the nanotube is made impossible when outer walls prevent it. This was shown for example in the case of the simultaneous filling of different kinds of nanotubes (SWNTs, DWNTs) where it was obvious in the case of the narrowest ones to crystallize PbI_2 within SWNTs, while this was impossible in DWNTs having the same inner diameter (Figure 5 (a, b)). [15]

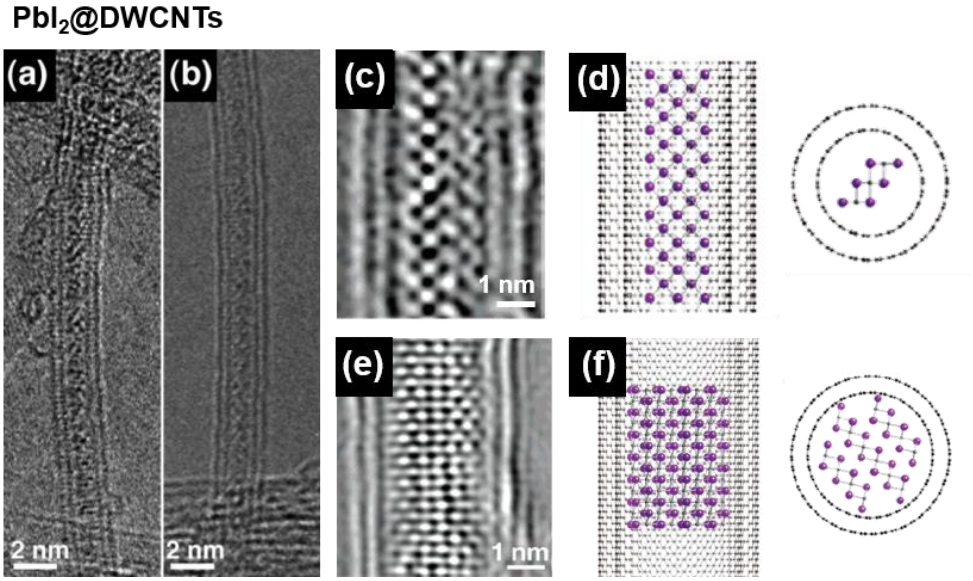

Figure 5. Structures of PbI_2 encapsulated within DWCNTs. (a) and (b) show two examples of HRTEM images obtained near to Scherzer defocus of narrow DWCNTs filled with noncrystallizing PbI_2. Phase images of 2H PbI_2 encapsulated within a double walled carbon nanotubes of (c) ca. 2 nm and (e) 2.5 nm-diameter accompanied by their respective side-on and end-on models (d) and (f). Adapted with permission from ref. [15], Copyright © 2006, American Chemical Society.

It was already mentioned that the synthesis method may play a role in both the filling yield and morphology of the inorganic nanoguest. When molten phase capillary wetting is employed for filling carbon nanotubes, the annealing temperature must be carefully selected, taking into account not only the melting temperature of the material but also whether it is susceptible to decompose, sublime, boil or undergo structural transitions. PbI_2 is a clear example of how not only the morphology of the host but also the conditions of the filling experiment can affect the resulting nanostructure after confinement into carbon nanotubes.

The layered structure of PbI_2 undergoes variations under thermal treatments, leading to the formation of at least three stable polytypes. When PbI_2 is encapsulated within CNTs at ca. 400 ºC the crystals show a clear selectivity to the formation of the 2H structure versus the 4H form. This is interesting because the temperature of treatment was enough to convert PbI_2 to its 4H polytype.[15]

In order to be confined inside a 1.6 nm diameter SWCNT, a fragment of an ideal 2D layer of PbI_2 might undergo a reduction of the coordination due to the removal of iodine atoms from the edges of the crystal formed by three chains of PbI_6 octahedra. This induces changes in the geometry of the crystal resulting in a structure with a central chain of PbI_6 octahedra surrounded by two chains of PbI_5 square pyramids. Experimental results match with the HRTEM simulation of the salt encapsulated within an equivalent nanotube (1.6 nm diameter). Narrower CNTs are able to accommodate the 2H structure, while one single specimen of the alternating form (4H stacking) was observed inside a wider carbon nanotube (2 nm).[15]

Additional structures of the 2H PbI_2 polytype can be grown by filling double-walled carbon nanotubes of larger inner dimensions. Phase images of the observed hybrids and their corresponding structural models are shown in Figure 5 (c-f). Increasing the inner diameter of the tube (2.5 nm) allows encapsulating three octahedral layers of PbI_2 with the crystal parallel to <121> with respect to its bulk form (e). Similar-sized nanotubes can encapsulate different microstructures due to variations of the orientation of the crystal. In both cases the <-210> reflections align parallel to the DWCNT axis, however the projections of the encapsulated crystals are viewed parallel to the non-equivalent <121> and <-1-21> directions, respectively.

Filling PbI_2 into CNTs with even larger diameters, i.e. MWCNTs, leads to the formation of single-layered PbI_2 nanotubes (PbI_2-NT). Figure 6 (a) shows a HRTEM image of a PbI_2-NT@MWCNTs as prepared by high temperature filling. A large variety of materials have been shown to also coat the inner cavities of MWCNT forming single-layered inorganic nanotubes (SLINTs), namely PbI_2,[57, 58] ZnI_2,[58, 59] $CeCl_3$,[59] CeI_3,[59] $TbCl_3$,[59] $GdCl_3$,[29] $SmCl_3$[29] BiI_3,[60] GdI_3[61] and $BiCl_3$.[62] The role

that the temperature of treatment has on the grown nanostructures was investigated using ZnI_2 and MWCNTs.[59] It was observed that the formation of SLINTs could be favored by increasing the temperature of treatments, reaching a selectivity of ca. 60 %. A much higher selectivity towards the formation of SLINTs has been recently reported using laser-assisted filling of PbI_2 inside MWCNTs (Figure 6 (b, c)). Not only the crystal structure, but also the optoelectronic properties of the material were found to change drastically upon encapsulation.[58]

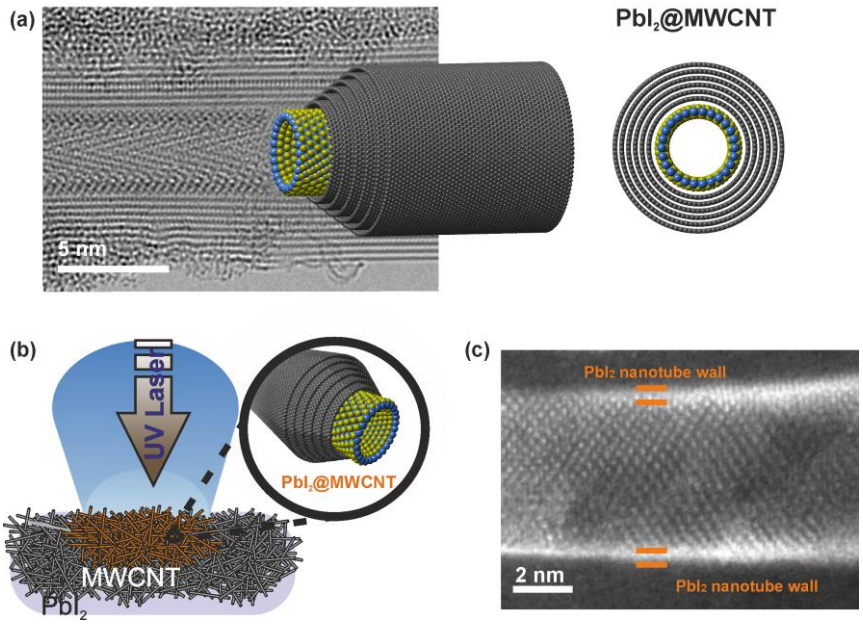

Figure 6. Single layered PbI_2 nanotubes encapsulated within MWCNTs. (a) HRTEM image of a sample prepared by conventional thermal annealing with the corresponding structural models. Adapted with permission from ref. [57], Copyright © 2013, John Wiley and Sons. (b) Schematic representation of laser-assisted filling of CNTs. (c) HAADF-STEM image of a single-layered PbI_2 nanotube grown inside MWCNTs by laser-assisted filling. Reprinted (adapted) with permission from ref. [58], Copyright © 2018, American Chemical Society.

From the examples illustrated above it becomes patent that not only the diameter of the hosting carbon nanotubes plays a major role on the amount of atoms that can be packed inside their inner cavities, but it also affects the interatomic distances and the distribution of those atoms along the crystalline structure. Since the atomic organization within the nanostructure is responsible of its chemical and physical characteristics, understanding the size-dependent building processes may allow the controlled tuning of

the properties of the guest structures. Paying special attention to this issue, both theoretical and experimental studies have been intended to understand the influence of the dimensions of the nanotubes in the structural characteristics of the final grown nanocrystal. Eliseev *et al.* observed three different nanostructures of PbTe, going from the bulk-like to lower dimensionality structures that can be distinguished within a small CNT diameter range (1.5 to 1.2 nm). When increasing the confining space (d = 1.32 nm) the material changes its crystallization direction to one with lower surface energy (from (110) to (100)); the increase in the atomic density results in a lower stability of the structure. More drastic variations are observed as decreasing the CNTs diameter which include redistribution of the atoms and changes in the stoichiometry leading to crystals which do not exist in the PbTe bulk form.[63] Wynn *et al.* also predicted the formation of energetically favorable nanowires of GeTe which structure is clearly ruled by the radius of the carbon nanotubes.[64] In the case of BiI_3, with a layered structure, a preferential formation of SLINTs against that of nanorods is observed when increasing the CNTs diameter.[60] The inorganic structural variations of the nanocrystals mentioned above are assigned to the influence of the inner diameter of the hosts, because according to theoretical calculations the chemical interaction and charge transfer between the crystals and the hosting nanotubes are thought to be negligible.

The presence of filling material inside CNTs also modifies their mechanical properties, and especially their resistance to applied pressure. This was investigated in many systems using Raman spectroscopy, especially in the case if DWCNTs filled with PbI_2,[65] Te [66] and Fe.[67] As illustrated in Figure 7, the pressure coefficient (expressed is $cm^{-1}.GPa^{-1}$) of the outer wall is larger than the one of the inner wall. This is already the case in empty DWCNTs.[68] However, the influence of the presence of nanocrystals within the nanotubes was clearly evidenced with a significant increase in

the slope (and thus an increase in the pressure coefficient) due to charge transfer between the guest and the host. No phase transformation of the guest was observed up to 11 GPa of applied pressure.

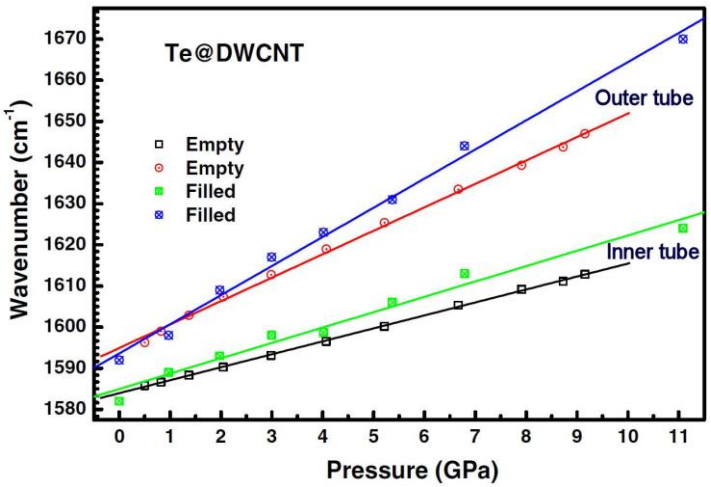

Figure 7. Pressure dependence of inner and outer shells of empty and Te-filled DWCNTs. Reprinted with permission from ref. [66], Copyright © 2010, American Chemical Society.

The temperature dependence of the frequency of the tangential modes of CNTs has also been evidenced (Se, Te, HgTe, PbI_2 [69]) to depend on the filling of the nanotubes, and can thus be used to demonstrate that CNTs are filled or empty, without requiring TEM observation. Charge transfer of CNTs due to doping effect was also evidenced by Raman spectroscopy in the case of filling with Iodine,[70, 71] leading to p-doping of the nanotubes. Figure 8 shows some illustrations of the high filling rate and variety of arrangement of iodine, which can be obtained through filling in the vapour phase.

Filling of CNTs was also proposed as an interesting way to tune the electrical transport properties of random assemblies of CNTs as already discussed earlier in the case of filling with Se or HgTe.[9] Finally, the magnetic properties of CNTs can also be modified through filling with magnetic compounds such as iron oxide of Gadolinium. In the case of iron oxide, superparamagnetic nanowires were stabilized within DWCNTs,[72] also leading to magneto-Coulomb effects.[73] DWCNTs Filled with Gadolinium exhibited Kondo effect and enhanced magnetic properties.[74, 75]

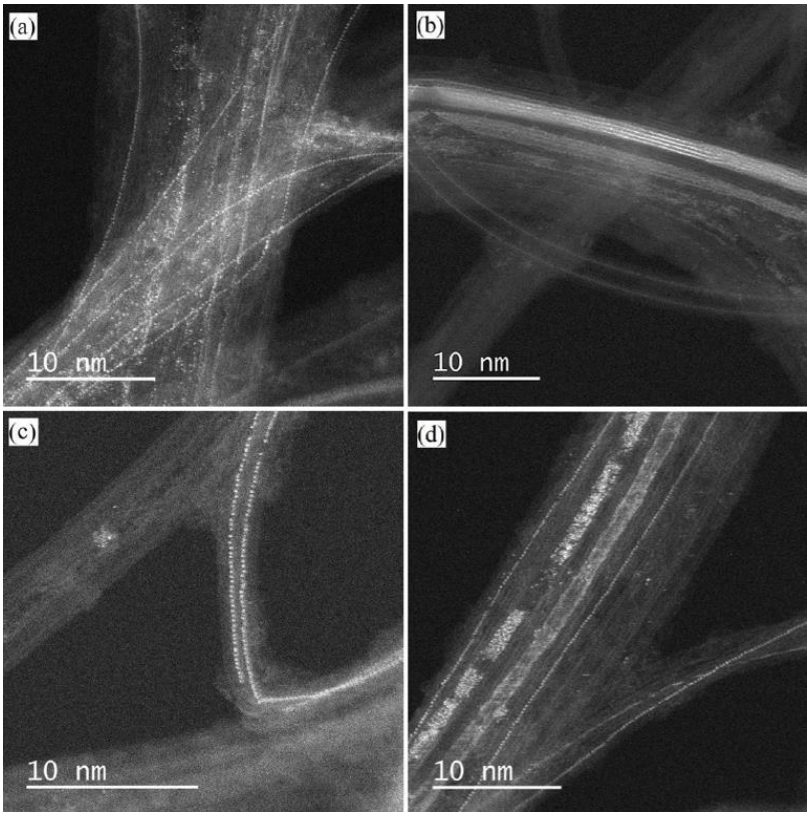

Figure 8. ***Annular Dark Field images (STEM operated at 200 kV) of I@DWNTs prepared from filling in the gas phase.*** *(a) Several single iodine chains (filling at 140°C), (b) two single iodine chains as wells as other structures in the background (filling at 140°C), (c) two single iodine chains (filling at 827°C), (d) several single iodine as well as other structures in the background (filling at 827°C). Reprinted with permission from ref. [76]. Copyright © 2017, IEEE.*

Encapsulation of inorganic crystals within CNTs is an attractive route for the template-assisted synthesis of new functional materials. CNTs not only act as moulds to control the dimensions of the new nanostructures, but also play a protective role, allowing the formation of nanostructures with a high interest due to their optical, chemical and electronic properties, but which stability at ambient conditions is extremely low.[77, 78] CNTs provide by themselves interesting characteristics to the new synthesized hybrids. Variations in the mechanical properties or induced electrical doping have been reported due to the interaction of both hosting nanotubes and inorganic crystals.[56] Thus, understanding the mechanisms of growth and interactions of the atoms from the encapsulated nanostructure with the conjugated lattice of the nanotubes is essential to develop new protocols for obtaining materials with specific properties and expanding

the range of applications. Using CNTs as template can lead to the formation of crystalline entities with different structures even when the same inorganic precursor is used. Thus, encapsulation within the cavities of CNTs can favour the formation of new low-dimensional allotropes[7] with special interest as semiconductors or sensors. Taking advantage of the versatility that the nanoencapsulation offers, CNTs can be used to prepare new hybrids with applications in nanoelectronics, optics and solar cells.[47, 79] CNTs can also be used as directing and protecting agents to carry reactions involving sensitive materials within their cavities (nanoreactors), in some cases in absence of catalyst or to control de size of the desired product,[80] thus opening up many possibilities to develop new strategies of synthesis.

Conclusions

Soon after the report of Iijima on carbon nanotubes back in 1991,[81] the possibility of filling their inner cavities was theoretically predicted by Pederson and Broughton.[82] On the following years several examples were published on the encapsulation of a variety of materials into multi-walled carbon nanotubes.[83] Prof. Malcolm L. H. Green, to whom this special issue is devoted, has performed an extensive research work regarding the filling of the inner channel of carbon nanotubes to synthesize unprecedented nanostructures, paving the way to many potential applications in a wide range of fields, from targeted drug delivery to sensors and nanoelectronics. The structure of the encapsulated material depends on the employed filling strategy, the diameter of the host and the host-guest interaction. Therefore, a given compound can adopt different structures when using CNTs as hosting templates. The revival of interest in this domain observed these recent years suggests that all the knowledge established so far will provide a strong basis for the understanding of the complex relationships between the host carbon nanotubes and guest compounds which can take the form of

nanoparticles, nanowires or even nanotubes. We hope it is clear from the short summary that the research in this field is at the interface between chemistry and materials science, requiring many modern analytical techniques and especially in the field of high-resolution TEM and associated tools such as dark-field imaging, EELS spectroscopy, and reconstruction from through focal series.

Acknowledgements

Emmanuel and Gerard would like to dedicate this work to Malcolm for all these years of support and inspiration. We acknowledge financial support from Spanish Ministry of Economy and Competitiveness through the "Severo Ochoa" Programme for Centres of Excellence in R&D (SEV-2015-0496), and CSIC PIE (201660E013).

References

[1] M. Martincic, G. Tobias, Expert opinion on drug delivery, 12 (2015) 563-581.
[2] C.J. Serpell, K. Kostarelos, B.G. Davis, ACS Central Science, 2 (2016) 190-200.
[3] J. Xiao, X. Pan, S. Guo, P. Ren, X. Bao, Journal of the American Chemical Society, 137 (2015) 477-482.
[4] R.H. Baughman, A.A. Zakhidov, W.A. de Heer, Science, 297 (2002) 787-792.
[5] M.V. Kharlamova, Progress in Materials Science, 77 (2016) 125-211.
[6] C. Xu, J. Sloan, G. Brown, S. Bailey, V.C. Williams, S. Friedrichs, K.S. Coleman, E. Flahaut, J.L. Hutchison, R.E. Dunin-Borkowski, M.L.H. Green, Chemical Communications, (2000) 2427-2428.
[7] M. Hart, J. Chen, A. Michaelides, A. Sella, M.S.P. Shaffer, C.G. Salzmann, Angewandte Chemie International Edition, 57 (2018) 11649-11653.
[8] S. van Bezouw, D.H. Arias, R. Ihly, S. Cambré, A.J. Ferguson, J. Campo, J.C. Johnson, J. Defillet, W. Wenseleers, J.L. Blackburn, Acs Nano, 12 (2018) 6881-6894.
[9] G. Chimowa, M. Sendova, E. Flahaut, D. Churochkin, S. Bhattacharyya, Journal of Applied Physics, 110 (2011) 123708.
[10] C.-C. Lin, B.T.T. Chu, G. Tobias, S. Sahakalkan, S. Roth, M.L.H. Green, S.-Y. Chen, Nanotechnology, 20 (2009) 105703.
[11] L. Cabana, M. Bourgognon, J.T.-W. Wang, A. Protti, R. Klippstein, R.T.M. de Rosales, A.M. Shah, J. Fontcuberta, E. Tobías-Rossell, J.K. Sosabowski, K.T. Al-Jamal, G. Tobias, Small, 12 (2016) 2893-2905.
[12] J.S. Bendall, A. Ilie, M.E. Welland, J. Sloan, M.L.H. Green, Journal of Physical Chemistry B, 110 (2006) 6569-6573.
[13] R. Ghunaim, C. Damm, D. Wolf, A. Lubk, B. Büchner, M. Mertig, S. Hampel, Nanomaterials, 8 (2018).
[14] P.V.C. Medeiros, S. Marks, J.M. Wynn, A. Vasylenko, Q.M. Ramasse, D. Quigley, J. Sloan, A.J. Morris, Acs Nano, 11 (2017) 6178-6185.
[15] E. Flahaut, J. Sloan, S. Friedrichs, A.I. Kirkland, K.S. Coleman, V.C. Williams, N. Hanson, J.L. Hutchison, M.L.H. Green, Chemistry of Materials, 18 (2006) 2059-2069.

[16] M. Monthioux, E. Flahaut, J.P. Cleuziou, Journal of Materials Research, 21 (2011) 2774-2793.
[17] C. Nie, A.-M. Galibert, B. Soula, E. Flahaut, J. Sloan, M. Monthioux, Carbon, 110 (2016) 48-50.
[18] S.C. Tsang, Y.K. Chen, P.J.F. Harris, M.L.H. Green, Nature, 372 (1994) 159-162.
[19] Y. K. Chen, A. Chu, J. Cook, M. L. H. Green, P. J. F. Harris, R. Heesom, M. Humphries, J. Sloan, S.C. Tsang, J. F. C. Turner, Journal of Materials Chemistry, 7 (1997) 545-549.
[20] J. Sloan, G. Matthewman, C. Dyer-Smith, A.Y. Sung, Z. Liu, K. Suenaga, A.I. Kirkland, E. Flahaut, ACS Nano, 2 (2008) 966-976.
[21] E. Dujardin, T.W. Ebbesen, H. Hiura, K. Tanigaki, Science, 265 (1994) 1850-1852.
[22] J. Sloan, D.M. Wright, H.G. Woo, S. Bailey, G. Brown, A.P.E. York, K.S. Coleman, J.L. Hutchison, M.L.H. Green, Chemical Communications, (1999) 699-700.
[23] Y.K. Chen, M.L.H. Green, S.C. Tsang, Chemical Communications, (1996) 2489-2490.
[24] M. Martincic, E. Pach, B. Ballesteros, G. Tobias, Physical Chemistry Chemical Physics, 17 (2015) 31662-31669.
[25] M. Kierkowicz, J.M. González-Domínguez, E. Pach, S. Sandoval, B. Ballesteros, T. Da Ros, G. Tobias, ACS Sustainable Chemistry & Engineering, 5 (2017) 2501-2508.
[26] B. Ballesteros, G. Tobias, M.A.H. Ward, M.L.H. Green, The Journal of Physical Chemistry C, 113 (2009) 2653-2656.
[27] G. Brown, S.R. Bailey, M. Novotny, R. Carter, E. Flahaut, K.S. Coleman, J.L. Hutchison, M.L.H. Green, J. Sloan, Applied Physics A, 76 (2003) 457-462.
[28] L. Shao, G. Tobias, Y. Huh, M.L.H. Green, Carbon, 44 (2006) 2855-2858.
[29] M. Martincic, S. Vranic, E. Pach, S. Sandoval, B. Ballesteros, K. Kostarelos, G. Tobias, Carbon, 141 (2019) 782-793.
[30] V. Sanz, C. Tilmacîu, B. Soula, E. Flahaut, H.M. Coley, S.R.P. Silva, J. McFadden, Carbon, 49 (2011) 5348-5358.
[31] P. Luksirikul, B. Ballesteros, G. Tobias, M.G. Moloney, M.L.H. Green, Carbon, 48 (2010) 1912-1917.
[32] L. Shao, T.W. Lin, G. Tobias, M.L.H. Green, Chemical Communications, (2008) 2164-2166.
[33] J. Sloan, M.C. Novotny, S.R. Bailey, G. Brown, C. Xu, V.C. Williams, S. Friedrichs, E. Flahaut, R.L. Callender, A.P.E. York, K.S. Coleman, M.L.H. Green, R.E. Dunin-Borkowski, J.L. Hutchison, Chemical Physics Letters, 329 (2000) 61-65.
[34] R.R. Meyer, J. Sloan, R.E. Dunin-Borkowski, A.I. Kirkland, M.C. Novotny, S.R. Bailey, J.L. Hutchison, M.L.H. Green, Science, 289 (2000) 1324-1326.
[35] W.K. Hsu, W.Z. Li, Y.Q. Zhu, N. Grobert, M. Terrones, H. Terrones, N. Yao, J.P. Zhang, S. Firth, R.J.H. Clark, A.K. Cheetham, J.P. Hare, H.W. Kroto, D.R.M. Walton, Chemical Physics Letters, 317 (2000) 77-82.
[36] J. Sloan, A.I. Kirkland, J.L. Hutchison, M.L.H. Green, Chemical Communications, 2 (2002) 1319-1332.
[37] J. Sloan, G. Brown, S.R. Bailey, K.S. Coleman, E. Flahaut, S. Friedrichs, C. Xu, M.L.H. Green, R.E. Dunin-Borkowski, J.L. Hutchison, A.I. Kirkland, R.R. Meyer, in, 2001, pp. A14311-A14316.
[38] J. Sloan, S.J. Grosvenor, S. Friedrichs, A.I. Kirkland, J.L. Hutchison, M.L.H. Green, Angewandte Chemie - International Edition, 41 (2002) 1156-1159.
[39] E. Philp, J. Sloan, A.I. Kirkland, R.R. Meyer, S. Friedrichs, J.L. Hutchison, M.L.H. Green, Nature Materials, 2 (2003) 788-791.
[40] N. Kuganathan, J.C. Green, Chemical Communications, (2008) 2432-2434.
[41] R. Carter, J. Sloan, A.I. Kirkland, R.R. Meyer, P.J.D. Lindan, G. Lin, M.L.H. Green, A. Vlandas, J.L. Hutchison, J. Harding, Physical Review Letters, 96 (2006) 215501.
[42] T.W. Chamberlain, J. Biskupek, G.A. Rance, A. Chuvilin, T.J. Alexander, E. Bichoutskaia, U. Kaiser, A.N. Khlobystov, Acs Nano, 6 (2012) 3943-3953.
[43] J. Zhang, Z. Zhu, Y. Feng, H. Ishiwata, Y. Miyata, R. Kitaura, E.P. Dahl Jeremy, M.K. Carlson Robert, A. Fokina Natalie, R. Schreiner Peter, D. Tománek, H. Shinohara, Angewandte Chemie International Edition, 52 (2013) 3717-3721.

[44] J. Zhang, D. Zhao, D. Xiao, C. Ma, H. Du, X. Li, L. Zhang, J. Huang, H. Huang, C.-L. Jia, D. Tománek, C. Niu, Angewandte Chemie, 129 (2017) 1876-1880.
[45] M. Hart, E.R. White, J. Chen, C.M. McGilvery, C.J. Pickard, A. Michaelides, A. Sella, M.S.P. Shaffer, C.G. Salzmann, Angewandte Chemie International Edition, 56 (2017) 8144-8148.
[46] M. Chorro, G. Kané, L. Alvarez, J. Cambedouzou, E. Paineau, A. Rossberg, M. Kociak, R. Aznar, S. Pascarelli, P. Launois, J.L. Bantignies, Carbon, 52 (2013) 100-108.
[47] N. Kuganathan, A. Chroneos, Inorganica Chimica Acta, 488 (2019) 246-254.
[48] E.L. Sceats, M.L.H. Green, A.I. Kirkland, J.C. Green, Chemical Physics Letters, 466 (2008) 76-78.
[49] D.G. Calatayud, H. Ge, N. Kuganathan, V. Mirabello, R.M.J. Jacobs, N.H. Rees, C.T. Stoppiello, A.N. Khlobystov, R.M. Tyrrell, E.D. Como, S.I. Pascu, ChemistryOpen, 7 (2018) 144-158.
[50] N.A. Kiselev, R.M. Zakalyukin, O.M. Zhigalina, N. Grobert, A.S. Kumskov, Y.V. Grigoriev, M.V. Chernysheva, A.A. Eliseev, A.V. Krestinin, Y.D. Tretyakov, B. Freitag, J.L. Hutchison, Journal of Microscopy, 232 (2008) 335-342.
[51] A.S. Kumskov, V.G. Zhigalina, A.L. Chuvilin, N.I. Verbitskiy, A.G. Ryabenko, D.D. Zaytsev, A.A. Eliseev, N.A. Kiselev, Carbon, 50 (2012) 4696-4704.
[52] A.A. Eliseev, N.I. Verbitskiy, A.A. Volykhov, A.V. Fedorov, O.Y. Vilkov, I.I. Verbitskiy, M.M. Brzhezinskaya, N.A. Kiselev, L.V. Yashina, Carbon, 99 (2016) 619-623.
[53] M.M. Brzhezinskaya, R. Püttner, A.S. Vinogradov, M.V. Chernysheva, A.A. Eliseev, N.A. Kiselev, A.V. Lukashin, Y.D. Tretyakov, Fullerenes, Nanotubes and Carbon Nanostructures, 18 (2010) 574-578.
[54] A.V. Generalov, M.M. Brzhezinskaya, A.S. Vinogradov, R. Püttner, M.V. Chernysheva, A.V. Lukashin, A.A. Eliseev, Physics of the Solid State, 53 (2011) 643-653.
[55] A.A. Eliseev, L.V. Yashina, N.I. Verbitskiy, M.M. Brzhezinskaya, M.V. Kharlamova, M.V. Chernysheva, A.V. Lukashin, N.A. Kiselev, A.S. Kumskov, B. Freitag, A.V. Generalov, A.S. Vinogradov, Y.V. Zubavichus, E. Kleimenov, M. Nachtegaal, Carbon, 50 (2012) 4021-4039.
[56] M.V. Kharlamova, C. Kramberger, O. Domanov, A. Mittelberger, K. Yanagi, T. Pichler, D. Eder, Journal of Materials Science, 53 (2018) 13018-13029.
[57] L. Cabana, B. Ballesteros, E. Batista, C. Magén, R. Arenal, J. Oró-Solé, R. Rurali, G. Tobias, Advanced Materials, 26 (2014) 2016-2021.
[58] S. Sandoval, D. Kepić, Á. Pérez del Pino, E. György, A. Gómez, M. Pfannmoeller, G.V. Tendeloo, B. Ballesteros, G. Tobias, ACS Nano, (2018).
[59] S. Sandoval, E. Pach, B. Ballesteros, G. Tobias, Carbon, 123 (2017) 129-134.
[60] A.E. Ashokkumar, A.N. Enyashin, F.L. Deepak, Scientific Reports, 8 (2018) 10133.
[61] N.M. Batra, A.E. Ashokkumar, J. Smajic, A.N. Enyashin, F.L. Deepak, P.M.F.J. Costa, The Journal of Physical Chemistry C, 122 (2018) 24967-24976.
[62] A. Ashok, L. Francis, A. Enyashin, Capillary filling of carbon nanotubes by BiCl3: TEM and MD insight, Nanosystems, physics, chemistry, mathematics, 2018.
[63] A.A. Eliseev, N.S. Falaleev, N.I. Verbitskiy, A.A. Volykhov, L.V. Yashina, A.S. Kumskov, V.G. Zhigalina, A.L. Vasiliev, A.V. Lukashin, J. Sloan, N.A. Kiselev, Nano Letters, 17 (2017) 805-810.
[64] J.M. Wynn, P.V.C. Medeiros, A. Vasylenko, J. Sloan, D. Quigley, A.J. Morris, Physical Review Materials, 1 (2017) 073001.
[65] J. González, C. Power, E. Belandria, J.M. Broto, P. Puech, J. Sloan, E. Flahaut, physica status solidi (b), 244 (2006) 136-141.
[66] E. Belandria, M. Millot, J.-M. Broto, E. Flahaut, F. Rodriguez, R. Valiente, J. Gonzalez, Carbon, 48 (2010) 2566-2572.
[67] J. González, C. Power, E. Belandria, J. Jorge, F. Gonzalez-Jimenez, M. Millot, S. Nanot, J.M. Broto, E. Flahaut, High Pressure Research, 28 (2008) 577-582.
[68] E. del Corro, J. González, M. Taravillo, E. Flahaut, V.G. Baonza, Nano Letters, 8 (2008) 2215-2218.
[69] M. Sendova, E. Flahaut, T. Hartsfield, Journal of Applied Physics, 108 (2010) 044309.

[70] T. Michel, L. Alvarez, J.L. Sauvajol, R. Almairac, R. Aznar, O. Mathon, J.L. Bantignies, E. Flahaut, Journal of Physics and Chemistry of Solids, 67 (2006) 1190-1192.
[71] A. Zubair, D. Tristant, C. Nie, D.E. Tsentalovich, R.J. Headrick, M. Pasquali, J. Kono, V. Meunier, E. Flahaut, M. Monthioux, I.C. Gerber, P. Puech, Physical Review Materials, 1 (2017) 064002.
[72] C.-M. Tîlmaciu, B. Soula, A.-M. Galibert, P. Lukanov, L. Datas, J. González, L.F. Barquín, J. Rodríguez Fernández, F. González-Jiménez, J. Jorge, E. Flahaut, Chemical Communications, (2009) 6664-6666.
[73] S. Datta, L. Marty, J.P. Cleuziou, C. Tilmaciu, B. Soula, E. Flahaut, W. Wernsdorfer, Physical Review Letters, 107 (2011) 186804.
[74] S. Ncube, C. Coleman, A. Strydom, E. Flahaut, A. de Sousa, S. Bhattacharyya, Scientific Reports, 8 (2018) 8057.
[75] S. Ncube, C. Coleman, A.S. de Sousa, C. Nie, P. Lonchambon, E. Flahaut, A. Strydom, S. Bhattacharyya, Journal of Applied Physics, 123 (2018) 213901.
[76] C. Nie, A. Galibert, B. Soula, L. Datas, J. Sloan, E. Flahaut, M. Monthioux, IEEE Transactions on Nanotechnology, 16 (2017) 759-766.
[77] L.V. Yashina, A.A. Eliseev, M.V. Kharlamova, A.A. Volykhov, A.V. Egorov, S.V. Savilov, A.V. Lukashin, R. Püttner, A.I. Belogorokhov, The Journal of Physical Chemistry C, 115 (2011) 3578-3586.
[78] L. Shi, K. Yanagi, K. Cao, U. Kaiser, P. Ayala, T. Pichler, Acs Nano, 12 (2018) 8477-8484.
[79] C.H. Chang, H. Jung, Y. Rheem, K.-H. Lee, D.-C. Lim, Y. Jeong, J.-H. Lim, N.V. Myung, Nanoscale, 5 (2013) 1616-1623.
[80] S. Heeg, L. Shi, L.V. Poulikakos, T. Pichler, L. Novotny, Nano Letters, 18 (2018) 5426-5431.
[81] S. Iijima, Nature, 354 (1991) 56-58.
[82] M.R. Pederson, J.Q. Broughton, Physical Review Letters, 69 (1992) 2689-2692.
[83] P.M. Ajayan, S. Iijima, Nature, 361 (1993) 333-334.